Hierarchically Constrained Dynamics and Emergence of Complex Behavior in Nanohybrids**

L. D. Carlos, J. M. Pacheco, R. A. S. Ferreira, and A. L. L. Videira*

Similar to living organisms, highly structured materials may manifest an inherent complexity, originating not only from their large number of core constituent units but also from the entanglement between the dynamics of the core components[1,2] and their organization as a complex multiagent system. As a result, such system typically exhibits properties that cannot be anticipated from those of their constituents. This, in turn, has provided experimental guidelines in investigating the relationship between the structural complexity and self-assembly mechanisms of nanostructured systems. Intriguingly, the potential role played by the complex organizing principles determining emergent physical phenomena has remained largely unexplored. In what follows, we provide experimental evidence and theoretical insight into the emergence of complex behavior in the context of an extended multiagent system made of an organic–inorganic nanostructured hybrid. Here, we show that the emitted relaxation energy of the nanohybrid upon repeated heating/cooling cycles exhibits a logarithmic time dependence, thereby providing a conspicuous fingerprint of emergent complex behavior; such logarithmic dependence has been associated with hierarchically constrained dynamics in many different multiagent systems. We employ a simple model to relate the individual dynamics in the nanohybrid with its hierarchical dependence on the system's collective dynamical features. The model associates the nanoscale interactions between the amide crosslinkages connecting the organic and inorganic components with the entire hybrid organization at the mesoscopic scale. The strong correlations between adjacent crosslinkages establish a memory effect – stemming from the hierarchical organization of the hybrid – inducing light emission, governed by the system-wide dynamics. As the model's underlying rationale is insensitive to the particulars of the specific multiagent analyzed, we propose that the emergence of complexity may be the rule, rather than the exception, in what concerns the interplay between individual and collective behavior.

Self-assembly of soft-matter components such as polymers, liquid crystals, surfactants, colloids and organic–inorganic hybrids may occur in regular, hierarchically organized structures.[3] Silsesquioxanes and organosilanes are examples in which ordered self-assembly architectures with well-defined morphologies at the macroscopic scale stem from the weak interactions between the organic spacers (hydrogen bonding, hydrophobic interactions, and π–π interactions).[4–8] Herein we consider the recently introduced self-assembled alkylene/siloxane hybrid nanostructure monoamidosil, henceforth named m-A(14), formed by highly ordered alkyl chains covalently crosslinked to siliceous nanodomains through amide bridges,[9] illustrated in Figure 1. In m-A(14), the self-assembly process arises from i) the intermolecular hydrogen bonding between the amide linkages, ii) an entropic contribution related to the structural phase separation between the organic and the inorganic domains, and iii) the van der Waals interactions between the polymer chains.

A reversible order–disorder phase transition of the alkylene chains is observed via a series of heating/cooling cycles operating between 296–393 K. The onset of this transition occurs at 363 K, involving a coherence length of 150 nm (≈30 times the distance $l = 5$ nm between the nanodomains).[9] The hydrogen-bonded amide–amide network, which involves ≈33 adjacent crosslinkages with a coherence length of ≈15 nm (Figure 1 and Supporting Information, Figure S1) begins to get disrupted at ≈340 K,[9] that is, before the onset of the order–disorder phase transition. Cooling the system down to room temperature reveals a slow kinetics of reformation – 10 to 100 hours, strongly temperature dependent – much slower than the characteristic time scale at which the phase transition occurs (a few minutes). The formation/annihilation of the hydrogen-bonded amide–amide network plays a central role in the emergence of complexity in m-A(14).

[*] Prof. L. D. Carlos, Dr. R. A. S. Ferreira
Departamento de Física, CICECO
Universidade de Aveiro
Aveiro, 3810-193 (Portugal)
E-mail: lcarlos@ua.pt
Prof. J. M. Pacheco
ATP-group, CFTC &
Departamento de Física da Faculdade de Ciências
P-1649-003 Lisboa (Portugal)
Prof. J. M. Pacheco, Prof. A. L. L. Videira
GADGET
Apartado 1329, 1009-001 Lisboa (Portugal)
Prof. A. L. L. Videira
R. Sarmento de Beires
31, 5 ESQ., 1900-411 Lisboa (Portugal)

[**] The authors thank V. de Zea Bermudez for the synthesis of the m-A(14) hybrid. L.D.C. thanks A. L. Ferreira and V. S. Amaral for fruitful discussions concerning the logarithmic time dependence. This work was supported by FEDER, FCT-Portugal through projects PTDC/CTM/72093/2006 and POCI/FIS/58418/04.

Supporting Information is available on the WWW under http://www.small-journal.com or from the author.

DOI: 10.1002/smll.200900899

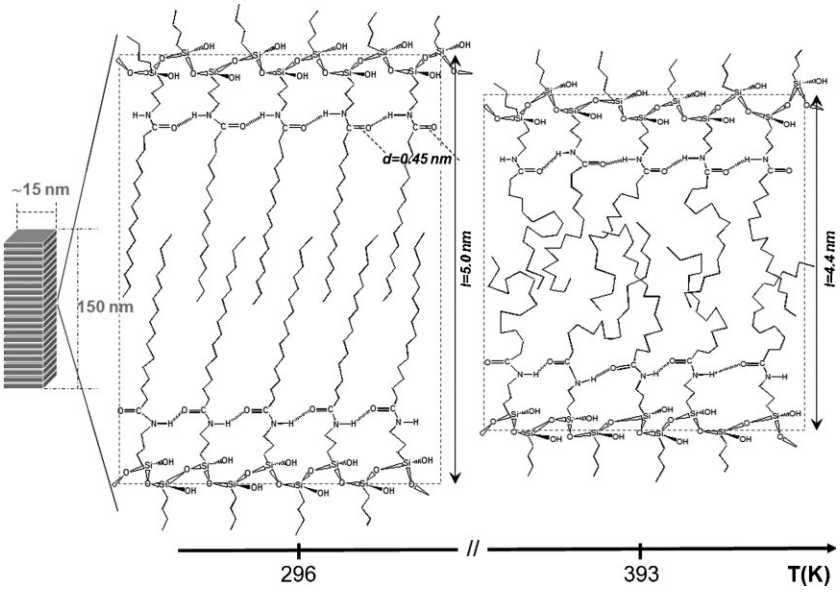

Figure 1. Structural illustration of the m-A(14) framework at 296 K and 393 K, illustrating the order–disorder phase transition.

Similar to what has been reported for other organic–inorganic hybrids,[10–14] m-A(14) is a room-temperature white-light emitter with a broad band spectrum, detailed in Figure 2, resulting from two contributions: a ''blue'' band (B), due to electron–hole recombinations in the NH/C=O groups of the amide crosslinkages (intensity peak in the B region of the spectra), and a ''purplish–blue'' band (PB), due to oxygen-related defects $^{\bullet}O-O-Si\equiv(CO_2)$ in the siliceous nanoclusters (with a maximum at higher energies in the PB region).[12,13] The spectra depicted in Figure 2, resulting from repeated heating/cooling cycles, exhibit a stronger temperature dependence in the B region – particularly above the onset of the amide–amide skeleton disruption – compared to the PB region. Furthermore, the peak value of the B-band energy at the beginning of the heating/cooling cycle is recovered, following a slow logarithmic time dependence of ≈300 hours[9] (Figure 3a). Consequently, the observed energy shift of the B-band peak energy back to its original value is associated with the restructuring of the H-bonded amide–amide skeleton, also responsible for the slow kinetics referred to before; as each of the individual intermolecular hydrogen bonds between adjacent amide linkages ($d = 0.45$ nm[9,14]) reforms, it favors the reformation of subsequent linkages within the range specified by the coherent length (≈15 nm). Remarkably, this process can be followed in detail via the emission spectra as it slowly recovers its reference value. Light emission originating from each nanostructure (amide crosslinkages) is therefore sensitive to the system-wide self-organization responsible for a thermally actuated ''memory effect''.

In Figure 3a we depict the time dependence of the relaxation of the B band, measured at five temperatures below the critical value of ≈340 K. A conspicuous effect emerges at intermediate times: the emitted energy scales

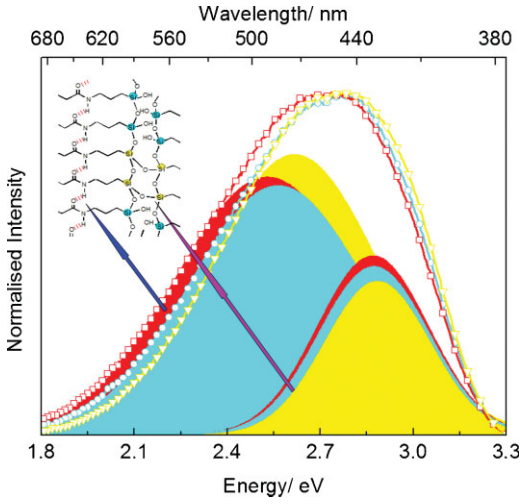

Figure 2. Emission spectra of the m-A(14) excited at 365 nm and recorded, on heating, at 296 (yellow), 373 (light blue), and 393 K (red). At each temperature, the spectra can be decomposed into the PB (right) and B (left) bands.

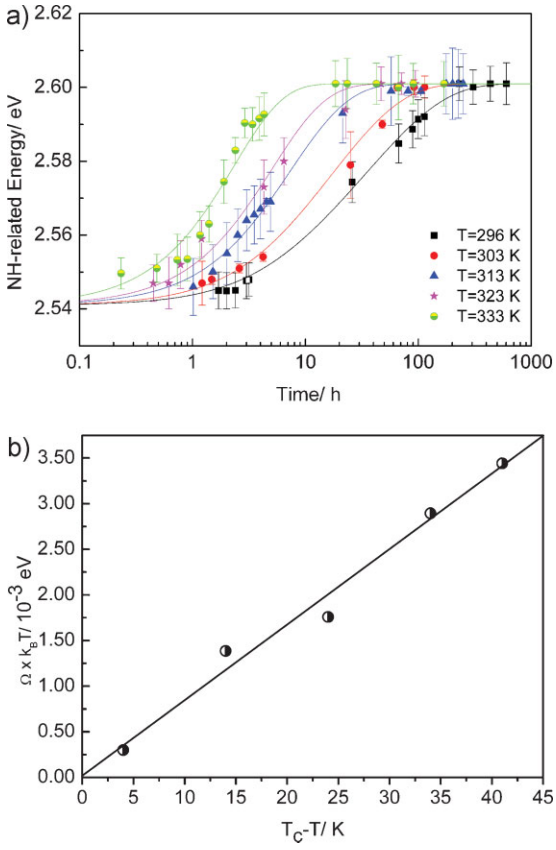

Figure 3. a) B-band relaxation of m-A(14). The solid colored lines are fits (reduced $\chi^2 = 0.372$) to the data using Equations (2) and (3). b) Temperature dependence of the optimal activation energy for fixed N. The solid line is a linear fit to the data ($T_C = 337$ K, $r = 0.991$).

logarithmically with time at all temperatures. Such a logarithmic regime with characteristic time scales of the order of 102 hours cannot be attributed to processes intrinsic to the atomic or molecular multiagents, which take place on much smaller characteristic time scales (see below); as a result, the time dependence of the light emitted from each individual component must reflect the detailed interplay between each of them and the system-wide structural organization taking place within the multiagent m-A(14) system. Such a logarithmic scaling has been recognized as a fingerprint of emergent complexity in several and disparate contexts, namely in the flux creep of type-II superconductors,[15] in magnetic relaxation in spin glasses,[15,16] in the kinetics of adsorption in granular materials,[17] in the structural relaxation of polymers,[18] in the chain-exchange kinetics of micelles,[19] in the local dynamics of DNA,[20] and in protein folding,[20,21] in all of which logarithmic variation in time has been associated with hierarchically constrained dynamics pointing to a proper time scale unrelated to their multiagents characteristic times. In the present case, the logarithmic time dependence of the B-band relaxation energy signals the emergent complexity arising from the strong correlation between the individual (optically active) amide bridges and the system-wide self-assembly, which ultimately determines the time scale of the relaxation energy stemming from each individual amide. That is, the NH/C=O related emission is not governed solely by its own complex mechanism independently of the others but rather by strongly correlated processes occurring at larger length scales associated with the formation/annihilation of the amide–amide array.

In what follows, we outlined a minimal model – inspired by a discussion of hierarchical constrained dynamics in complex systems by Palmer et al.[22] and Brey and Prados[16] – which establishes a relation between individual dynamics in a multiagent system and its hierarchical dependence on the collective dynamical pattern. We now examine how the model applies to m-A(14), showing, in particular, how the model relates the light emission of individual amide bridges with its dependence on the overall self-assembly dynamics of this multiagent nanohybrid. Let us consider a system composed of N multiagents, each of which may be in one of two states, an uncoupled state $|1>$ with energy E_1 and a coupled state $|0>$ with energy E_0. We assume that

a) Initially ($t = 0$), the N multiagents are uncorrelated, that is, all of them are in state $|1>$. Let $n(t)$ specify the number of multiagents in $|1>$ at time t. As $t \to \infty$, all the N multiagents will eventually relax into the fully correlated state $|0>$. Hence $n(0) = N$ and $n(t \to \infty) = 0$.
b) In each $|1> \to |0>$ transition of one of the multiagents, the same amount of energy ΔE is released.
c) Hierarchical condition: the probability of occurrence of the $|1> \to |0>$ transition depends on the number of transitions that have already taken place before (hierarchical memory effect). Denoting this transition probability by W, we may write $W_{n+1} = W_n e^{-\Omega(N,T)}$, where $\Omega(N,T)$ measures the strength of the correlation of the multi-agent system, which we expect to depend on the temperature T and the number N of agents.

Given this hierarchical condition for the transition probabilities W_k, we define the average lifetime of k-correlated multiagents as, $\tau_k = {W_k}^{-1} = \tau_0 \exp(k\Omega)$, $k = 0,\ldots, N$, with τ_0 characterizing the time scale of each $|1> \to |0>$ transition in the fully uncorrelated regime (in particular $\tau_N >> \tau_0$)[22]. Ω varies with the temperature at which the $|1> \to |0>$ transition occurs, as it manifests the degree of correlation between the multiagents; thus, at temperatures high enough to wash out correlation between agents, $\Omega \to 0$, and all transition rates are characterized by τ_0. Also, $\Omega \to 0$ as $N \to 0$, indicating that, below a minimum value of multi-agents, the disorder–order transition never occurs. We introduce the relaxation quantity:

$$\phi(t) = \frac{n(t) - n(t \to \infty)}{n(0) - n(t \to \infty)} = [n(0) = N \wedge n(t \to \infty) = 0] = \frac{n(t)}{N} \qquad (1)$$

such that $\phi(t = 0) = 1$, $\phi(t \to \infty) = 0$. Since every time a transition takes place an amount of energy $\Delta E$is released, the energy variation in time of the system, $E(t)$, ranges from a minimum value E_0 to a maximum value $N\Delta E$, and may be expressed as:

$$E(t) = E_0 + [N - n(t)]\Delta E = E_0 + N\Delta E[1 - \phi(t)] \qquad (2)$$

such that knowledge of $\phi(t)$ allows us to predict the shape of $E(t)$. For $\phi(t)$ we may write:[16]

$$\begin{aligned}\phi(t) &= \frac{2}{N+1}\sum_{k=0}^{N}\frac{k}{N}\exp\left\{-\frac{t}{\tau_k}\right\} \\ &= \frac{2}{N+1}\sum_{k=0}^{N}\frac{k}{N}\exp\left\{-\frac{t}{\tau_0}e^{-k\Omega(N,T)}\right\}\end{aligned} \qquad (3)$$

The nonlinear least-squares fits to the relaxation energies of the B component, based on Equations (2) and (3), are depicted as solid lines in Figure 3a. The initial values of τ_0 and Ω were varied by one order of magnitude to ensure that no bias in the final values was introduced. Attending to the uncertainty of the experimental E_0, ΔE, and N input values, the error in the fitted parameter values is ≈10%. The optimization variable was the reduced χ^2 error in the emission energy peak values (acceptable fits correspond to reduced χ^2 values smaller than 1). For m-A(14), we have $E_0 = 2.541 \pm 0.001$ eV, $N\Delta E = 0.060 \pm 0.001$ eV, with $N = 33 \pm 3$; the characteristic time scale of emission from a single (uncorrelated) agent, τ_0, and the correlation strength, Ω, remain adjustable parameters. From our fits – and in accordance with the present model – we get a temperature-independent τ_0 of 1.75 hours and a temperature dependence for Ω (for fixed N), shown in Figure 3b for the product $\Omega \times k_B\, T$ as a function of $T_C - T$, with $T_C = 337$ K, the critical temperature at which we find that $\Omega = 0$. This critical value is in excellent agreement with the onset of the disruption of the amide–amide network, above which one expects that correlations no longer play a significant role. On the other hand, at temperatures lower than 296 K, Ω must saturate, when the amide–amide array attains its maximum degree of correlation (which we expect to depend on N). Therefore, $\Omega > 0$ mirrors the conditions under which the

Final page numbers not assigned

emergent complex behavior of m-A(14) – resulting from the self-organization of its multiagents – is stable. In other words, the parameter Ω measures indeed the strength of the correlated state, a feature that depends on T and N, and that must be adequately specified, depending on the problem under study.[16,21]

The agreement between the model and the experimental data can be further assessed by comparing, in particular, the experimental and the fitted $t_{1/2}$ values ($t_{1/2}$ defined as the time at which the energy of the B-component has relaxed to half of its initial value – Figure 3a). For example, the experimental and fitted $t_{1/2}$ values deviate by ≈3% at 333 K and ≈10% at 296 K, respectively.

In the case of m-A(14), it is convenient to interpret Ω as an energy ratio between a thermal activation energy $\Delta\varepsilon$ and the thermal energy $k_B T$ at which cooling takes place. Hence, at each cooling temperature T, the quantity $\Omega \times k_B T$ in Figure 3b corresponds to such an activation energy; the values obtained and the linear behavior, in turn, correlate nicely with the thermal energy difference between the cooling temperature and the decorrelation temperature of $T_C = 337$ K, at which value the linear fit intercepts zero. This reinforces the idea that increasing temperature destroys the system-wide overall coherence, such that a qualitative measure of the correlation energy of the system may be provided in terms of an activation energy.

In summary, the m-A(14) hybrid contains single agents (amide crosslinkages) exhibiting an individual behavior, when isolated, which is markedly different from the one they manifest when embedded in the complex nanostructure. In the same fashion, many different examples abound in nature where multiagents constrained by simple rules can – by means of the symbiotic mechanisms of cooperation between them – generate the emergence of complex characteristics in the resulting structure. In the nonliving world, such is the case of the prototype for nonlinear chemical dynamics, the Belousov–Zhabotinsky (BZ) reactions.[23] In living organisms, we may take as examples foraging, nest building, and exploration of new areas by hymenoptera,[24–28] or the metabolic rate of mammalian cells.[29] The foraging dynamic pattern of a single individual, or the cell metabolic rate in vitro, are qualitatively independent of the colony or of the organism of origin, unlike the corresponding pattern of an individual taken collectively as a member of the colony or the metabolic rate in vivo, both ultimately dictated by the complex organism.

The fact that for m-A(14) the system-wide organization depends on the number N of amide–amide bridges and on the temperature T at which the relaxation occurs after cooling has correspondence in other cases. Thus, for the BZ reactions, collective (periodic) patterns are temperature dependent and are only observed for sufficiently high concentrations of reactants,[23] illustrating the dependence of the order–disorder phase transition on the temperature and the number of multiagents (concentration of reactants).

While for m-A(14) the temperature acts as a stimulus favoring the transition between an ordered and disordered pattern, for ants, this transition is mediated by a pheromone trail: ''a large colony size favors phase transition between disordered and ordered collective behavior''.[24,25] That is, larger colonies (multicomponent agents) should exhibit stronger correlations than smaller ones, such that below a minimum value of nestmates, the ants forage in a disorganized manner (as the pheromone concentration in each trails decreases). Likewise, bee societies are now considered self-organized complex adaptive multiagent systems, functioning as ''a mammal in many bodies''.[28] The hierarchical mechanisms of honey bees (*Apis mellifera*) that led to the emergence of coherence in a beehive have been painstakingly teased out.[26,27] Thus, for example, when looking for a new location for a colony, bees who had discovered possible adequate sites advertise their findings to the hive by dancing to her nestmates. The more highly a location is considered to be by a given bee (the stimulus enhancing the decision taking, equivalent to the temperature for m-A(14)), the more supporters it gains, to the point where the best choice wins over and the swarm occupies it (when a phase transition occurs). Also, the metabolic rates of single cells isolated from mammals of different body sizes converge towards a common value, rather than scaling with the organism size (body mass, encompassing eight orders of magnitude), as exhibited when correlated in the whole organism.[29] Here, in vivo dynamics of ''correlated cells'' result from the highly constrained hierarchical organization of energy transport cellular networks (the stimulus corresponding to temperature) that brings about the power-law decrease of their energy production rates with their body mass (number of multiagents).

Experimental Section

Photoluminescence spectroscopy: Emission spectra were recorded on a Fluorolog-3 (model FL3-2T) with a double-excitation spectrometer and a single-emission spectrometer (TRIAX 320), coupled to a R928 photomultiplier, using the front-face acquisition mode. The excitation source was a 450 W Xenon lamp. Emission was corrected for the spectral response of the monochromators and the detector using the typical correction spectrum provided by the manufacturer. The temperature was varied using an IES-RD31 controller and a Kapton® thermofoil heater from Minco, mounted on a Cu holder.

Fitting procedure: The fitting procedure (simultaneously applied to all curves) was performed using the Nelder–Mead nonlinear least squares algorithm implemented using the *MatLab*® optimization toolbox.

Keywords:

complexity · nanohybrids · organic–inorganic hybrids · self-assembly

[1] R. B. Laughlin, D. Pines, *Proc. Natl. Acad. Sci. USA* **2000**, *97*, 28–31.
[2] J. M. Lehn, *Rep. Prog. Phys.* **2004**, *67*, 249–265.
[3] K. Valle, P. Belleville, F. Pereira, C. Sanchez, *Nat. Mater.* **2006**, *5*, 107–111.
[4] A. Shimojima, D. Mochizuki, K. Kuroda, *Chem. Mater.* **2001**, *13*, 3603–3609.
[5] B. Boury, R. Corriu, *Chem. Rec.* **2003**, *3*, 120–132.

[6] J. J. E. Moreau, B. P. Pichon, M. W. Chi-Man, C. Bied, H. Pritzkow, J.-L. Bantignies, P. Dieudonné, J.-L. Sauvajol, *Angew. Chem. Int. Edit.* **2004**, *43*, 203–206.
[7] I. Karatchevtseva, D. J. Cassidy, M. Wong Chi Man, D. R. G. Mitchell, J. V. Hanna, C. Carcel, C. Bied, J. J. E. Moreau, J. R. Bartlett, *Adv. Funct. Mater.* **2007**, *17*, 3926–3932.
[8] A. Shimojima, C. W. Wu, K. Kuroda, *J. Mater. Chem.* **2007**, *17*, 658–663.
[9] L. D. Carlos, V. de Zea Bermudez, V. S. Amaral, S. C. Nunes, N. J. O. Silva, R. A. S. Ferreira, J. Rocha, C. V. Santilli, D. Ostrovskii, *Adv. Mater.* **2007**, *19*, 341–348.
[10] W. H. Green, K. P. Le, J. Grey, T. T. Au, M. J. Sailor, *Science* **1997**, *276*, 1826–1828.
[11] L. D. Carlos, V. de Zea Bermudez, R. A. Sá Ferreira, L. Marques, M. Assunção, *Chem. Mater.* **1999**, *11*, 581–588.
[12] L. D. Carlos, R. A. S. Ferreira, V. de Zea Bermudez, S. J. L. Ribeiro, *Adv. Funct. Mater.* **2001**, *11*, 111–115.
[13] L. D. Carlos, R. A. S. Ferreira, R. N. Pereira, M. Assunção, V. de Zea Bermudez, *J. Phys. Chem. B* **2004**, *108*, 14924–14932.
[14] S. S. Nobre, C. D. S. Brites, R. A. S. Ferreira, V. de Zea Bermudez, C. Carcel, J. J. E. Moreau, J. Rocha, M. W. Chi–Man, L. D. Carlos, *J. Mater. Chem.* **2008**, *18*, 4172–4182.
[15] P. E. Anderson, H. J. Jensen, L. P. Oliveira, P. Sibani, *Complexity* **2004**, *10*, 49–56.
[16] J. J. Brey, A. Prados, *Phys. Rev. E* **2001**, *63*, 021108–4.
[17] L. Bocquet, E. Charlaix, S. Ciliberto, J. Crassous, *Nature* **1998**, *396*, 735–737.
[18] A. Arbe, A.-C. Genix, J. Colmenero, D. Richter, P. Fouquet, *Soft Matter* **2008**, *4*, 1792–1795.
[19] R. Lund, L. Willner, J. Stellbrink, P. Lindner, D. Richter, *Phys. Rev. Lett.* **2006**, *96*, 068302–4.
[20] E. B. Brauns, M. L. Madaras, R. S. Coleman, C. J. Murphy, M. A. Berg, *Phys. Rev. Lett.* **2002**, *88*, 158101–158104.
[21] E. Abrahams, *Phys. Rev. E* **2005**, *71*, 051901–4.
[22] R. G. Palmer, D. L. Stein, E. Abrahams, P. W. Anderson, *Phys. Rev. Lett.* **1984**, *53*, 958–961.
[23] F. Sagues, I. R. Epstein, *Dalton Trans.* **2003**, *7*, 1201–1217.
[24] A. Dussutour, V. Fourcassie, D. Helbing, J. L. Deneubourg, *Nature* **2004**, *428*, 70–73.
[25] C. Detrain, J. L. Deneubourg, *Phys. Life Rev.* **2006**, *3*, 162–187.
[26] M. Lindauer, *Communication Among Social Bees*, 2nd Ed. Harvard University Press, Cambridge, MA **1971**.
[27] T. D. Seeley, P. K. Visscher, *Apidologie* **2004**, *35*, 101–116.
[28] J. Tautz, in *Biology of a Superorganism*, Springer, Berlin **2008**.
[29] G. B. West, W. H. Woodruff, J. H. Brown, *Proc. Natl. Acad. Sci. USA* **2002**, *99*, 2473–2478.

Received: May 27, 2009
Published online:

